Wood Science and Technology (2019) 53:1111–1134
https://doi.org/10.1007/s00226-019-01122-y

ORIGINAL

Assessing internal soundness of hardwood logs through acoustic impact test and waveform analysis

Feng Xu[1] · Yunfei Liu[1] · Xiping Wang[2] · Brian K. Brashaw[2] · Lon A. Yeary[3] · Robert J. Ross[2]

Received: 4 March 2019 / Published online: 13 September 2019

Abstract
The objective of this study was to explore the potential of an acoustic impact test as a nondestructive evaluation procedure to assess the soundness of hardwood logs in terms of internal decay, void, and defect ratio. Fifteen logs of four hardwood species (black cherry, white oak, red oak, and cottonwood) were obtained and subjected to acoustic impact testing. The logs were subsequently dissected for visual examination and physical mapping of the internal defects. The acoustic response signals were analyzed to derive acoustic velocity (through FFT), time centroid (through moment analysis), and the first- and second-order damping ratio (through continuous wavelet transform). The longitudinal acoustic velocity was found to have a negative, nonlinear relationship with defect ratio ($R^2=0.72$), but it lacked sensitivity to small defects and was affected by species. Time centroid proved to be a better predictor than acoustic velocity with an improved correlation with log defect ratio ($R^2=0.87$). Wavelet-based damping ratio was found to have a close linear relationship with log defect ratio. Comparing with the first-order damping ratio, the second-order damping ratio had a better predicting power ($R^2=0.92$) and was not affected by type and location of defects. The results further indicated that a combination of acoustic velocity, time centroid, and the first- and second-order damping ratios could yield the optimal prediction of log defect ratio. However, considering the sensitivity and simplicity of the waveform analysis, the second-order damping ratio of the response

✉ Yunfei Liu
lyf@njfu.com.cn

✉ Xiping Wang
xiping.wang@usda.gov

Extended author information available on the last page of the article

signals could be the best single predicting parameter for assessing the internal soundness of hardwood logs.

Introduction

Internal defects such as decay, void, and internal cracks are common in sawn logs of many hardwood species. Processing sawn logs with hidden internal defects can cause significant monetary loss to hardwood industry as a result of low board recovery and low-grade yield. Early detection of internal log defects can help to improve sawing procedures and maximize the board recovery (Thomas 2008, 2010). Research has shown that the value of hardwood lumber can be improved as much as 10–21% if internal defect information in hardwood logs such as location, type, size, and shape is used efficiently during the sawing process (Steele et al. 1994; Thomas 2010).

Acoustic technologies have been well established as material evaluation tools in the past several decades and are becoming widely accepted in the forest products industry for online quality control and product grading (Wang et al. 2007). For example, acoustic velocity as a nondestructive measure has been proved to be related to the basic wood and fiber properties such as stiffness, density, micro-fibril angle, and cellulose (Carter et al. 2005; Wang et al. 2007, 2013; Essien et al. 2017). It has also been recognized as a predicting parameter for wood deterioration caused by any wood decay mechanism (Pellerin et al. 1985; Ross et al. 2005). However, most of the predictive parameters, including acoustic velocity, transmission time, attenuation, etc., are derived from time or frequency domain analysis of the acoustic signals, and they offer limited information regarding internal quality features in terms of soundness and natural structural defects. Field application of acoustic sorting technology has been mostly found in softwood mills where logs, poles, and lumber are evaluated for global stiffness (Addis et al. 1997, 2000; Carter and Lausberg 2003; Huang et al. 2003; Carter et al. 2005; Wang et al. 2013). Research on the use of acoustic methods for detecting internal defects and grading hardwood logs is very limited. In a mill study, Wang et al. (2004) explored the use of longitudinal stress wave transmission time to sort red maple logs for structural quality. Although positive relationships were reported between log stress wave grades and lumber yield and average lumber stiffness, no attempt was made to investigate the impact of specific types of defects on acoustic measures. Later on in a large-scale mill study, Wang et al. (2009) further tested the feasibility of using a resonance acoustic technique to assess the extent of borer infestation in red oak logs affected by oak decline. The primary defects associated with the borer infestation included decay, incipient decay, grub holes, worm holes, and mineral streak. The key acoustic parameter examined in this study was acoustic velocity. The results revealed good positive relationships between log acoustic velocity and the yield of high-quality boards; and negative relationships were found between log acoustic velocity and the yield of low-quality boards.

Limited research has indicated that physical and structural damages, on both macro- and micro-structural level, could have a significant impact on the acoustic wave properties measured in hardwood logs. However, the accuracy of acoustic sorting applied to hardwood logs is far from desired. Research is needed to explore new acoustic features beyond acoustic velocity to assess hardwood logs in terms of internal defects and board visual criteria.

This study is part of a collaborative research program between the USDA Forest Service and the University of Minnesota Duluth to examine the technical feasibility of combining acoustic wave data with high-resolution laser scanning data to improve accuracy of hardwood log defect detection (Xu et al. 2018; Wang et al. 2018). The objective of this laboratory investigation was focused on exploring the information within the acoustic signals of hardwood logs using continuous wavelet transform (CWT) and identifying new signal features for assessing the internal soundness of hardwood logs. Log samples of four northern hardwood species of the Great Lakes region were obtained and used in this investigation. Acoustic impact testing was used to obtain response signals from each log. The logs were subsequently dissected for visual examination and physical mapping of the internal defects. The acoustic response signals were analyzed to derive acoustic velocity (through FFT), time centroid (through moment analysis), and the first- and second-order damping ratio (through continuous wavelet transform). These acoustic parameters were then correlated against the soundness of the logs in terms of internal decay, void, and defect ratio. This paper is based on a previous presentation (Xu et al. 2017) with significant revisions and additions.

Materials and methods

Fifteen mill-length logs of mixed hardwood species were obtained from a local wood company in Madison, Wisconsin, USA, for this study. The log specimens included two black cherries (*Prunus serotina* Ehrh.), five white oaks (*Quercus alba* L.), six red oaks (*Quercus rubra* L.), and two cottonwoods (*Populus deltoides* Bartr. ex Marsh.). These logs were selected from the company's log stocks based on visual appearances so that they included both sound and unsound logs. The unsound logs had a range of defects (voids, cracks, ring shake, internal decay, etc.) and were in different deterioration levels. Upon delivery to the USDA Forest Service, Forest Products Laboratory, the logs were placed on the ground inside a building prior to testing. Each log was assigned a log number, and the basic dimensions were measured. Table 1 shows the species information and dimensions of the logs.

Experimental procedures

Acoustic impact test (longitudinal direction)

All logs were first subjected to acoustic impact tests in longitudinal directions. Acoustic impact tests were conducted in two different ways: (1) using a handheld resonance acoustic tool (Hitman HM200, Fibre-gen, Inc., Auckland, New Zealand) to directly measure the acoustic velocity of each log and (2) using a laboratory

Table 1 Physical characteristics of the hardwood logs

Log no.	Species	Length (m)	Diameter (D) (cm)						MC (%)	Defects observed	Defect ratio k (%)
			D_L^a		D_S^b		Average				
							D_L	D_S			
1	Black cherry	2.44	45.4	39.1	38.0	38.1	42.2	38.1	48.4	Solid	0
2	Red oak	2.54	54.0	53.3	40.6	38.7	53.7	39.7	39.7	Rot, void, crack, hole	28.6
3	White oak	2.62	38.6	38.1	38.4	28.6	38.3	33.5	80.8	Void, crack, decay ring shake	14.6
4	Red oak	2.49	34.1	25.6	23.2	20.6	29.9	21.9	61.6	Void, decay, crack, knot	6.9
5	Black cherry	2.62	48.6	43.2	44.3	38.6	45.9	41.4	58.3	Crack, void	4.6
6	White oak	2.48	38.1	35.9	33.0	33.0	37.0	33.0	31.3	Void	31.7
7	Red oak	2.67	61.9	59.2	51.8	51.4	60.6	51.6	75.9	Void	6.4
8	Cottonwood	2.60	36.2	35.6	35.7	35.6	35.9	35.6	95.6	Ring shake	0
9	Red oak	2.53	51.4	45.7	43.5	41.0	48.6	42.2	86.0	Void, knot, hole	15.1
10	White oak	2.46	31.0	30.6	26.0	23.8	30.8	24.9	52.5	Void, split, twist	13.5
11	White oak	2.55	55.7	50.8	38.1	37.8	53.3	37.9	77.4	Void	20.3
12	White oak	2.34	38.9	35.6	31.1	30.5	37.2	30.8	46.6	Extensive checks, rot, knot	5.4
13	Cottonwood	2.44	33.0	31.4	31.4	28.1	32.2	29.8	76.8	Surfaces decay, split, heartwood decay	8.0
14	Red oak	2.59	38.4	38.1	35.9	35.6	38.3	35.7	68.8	Void, internal crack	10.0
15	Red oak	2.64	44.0	39.2	45.5	43.5	41.6	44.5	70.3	Split, internal crack, broken pieces, knot	3.7

[a,b] D_L and D_S are for the diameters of large end and small end, respectively

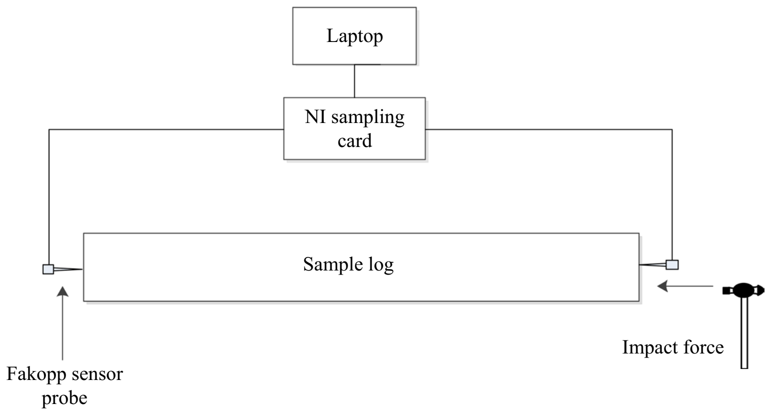

Fig. 1 Acoustic impact test (longitudinal direction) in a log to obtain and record response signals

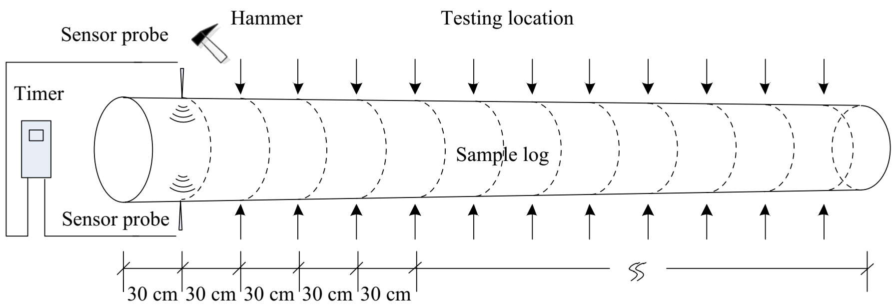

Fig. 2 Schematic diagram of stress wave transit time measurements (radial direction) in a log

impact testing system to obtain and record the response signals from each log following a mechanical impact.

To collect the response signals from each log, two sensor probes (Fakopp spike sensors, Fakopp Enterprise Bt., Agfalva, Hungary) were inserted into the opposing ends of each log near the geometric center as shown in Fig. 1. The acoustic waves were generated through a medium-sized hammer (680 g), i.e., the hammer of HM200 tool, impact at one end. The response signals were recorded through a data acquisition card (NI 5132) connected to the laptop, with a sampling frequency of 20 kHz and a sampling length of 2000 points.

Stress wave transit time (SWTT) measurements (radial direction)

Following the impact test, a series of stress wave transmission tests were conducted on each log in the radial direction using a Fakopp Microsecond Timer (Fakopp Enterprise Bt., Agfalva, Hungary), starting from the cross section 30 cm from the large end and at cross sections with a 30 cm increment throughout the entire length of each log (Fig. 2). Detailed procedures for SWTT measurements can be found in

Wang et al. (2005). In this study, the stress wave transit times measured in the radial direction were used to assess the physical conditions at various locations of each log. The transit time distribution in each log was then used to determine the dissecting locations in order to reveal the internal defects.

Dissecting logs and ground-truth defect mapping

Upon completion of the nondestructive tests, each log was radially dissected at locations where internal defect was indicated by the mapping of stress wave transit time (SWTT). As an example, Fig. 3 illustrates the dissecting locations for log no. 7 (red oak) assisted with the SWTT data. Visual inspection and physical measurements were then conducted at each opened cross section to determine the locations and sizes of the defects (voids and decay). Based on the measurements of defect areas on dissected cross sections and their extended lengths, a ground-truth defect map was created for each log (Fig. 3b). The percentage of the compromised wood in each log, defined as defect ratio, was subsequently determined by dividing the volume of defect areas by the total log volume.

Determination of log moisture content (MC)

To determine the moisture levels of the logs, one to two 5-cm-thick disks were cut from each log at least 30 cm from the log ends. The moisture content (MC) of each disk was determined using oven dry method in accordance with the ASTM Standard D4442-92 (ASTM 2003).

Feature extraction of acoustic signals

Comparing the waveforms of response signals received from the impact end and the opposite end (Fig. 4), it was found that the main frequency components of both signals

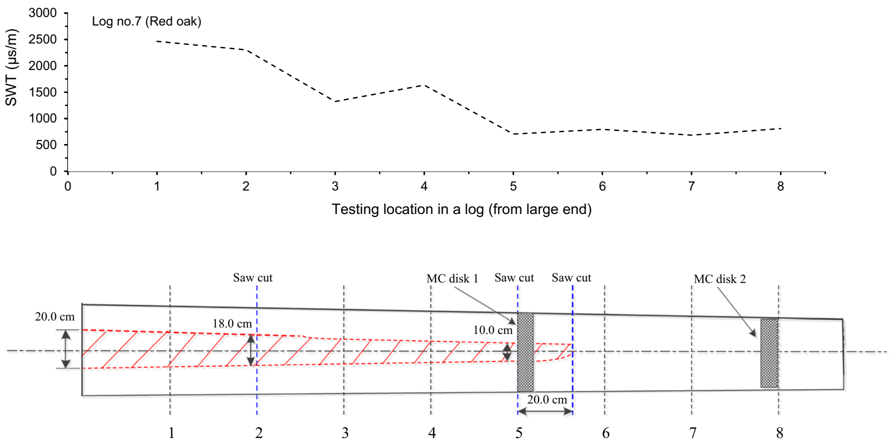

Fig. 3 Illustration of dissecting hardwood log samples and defect mapping (log no. 7—red oak)

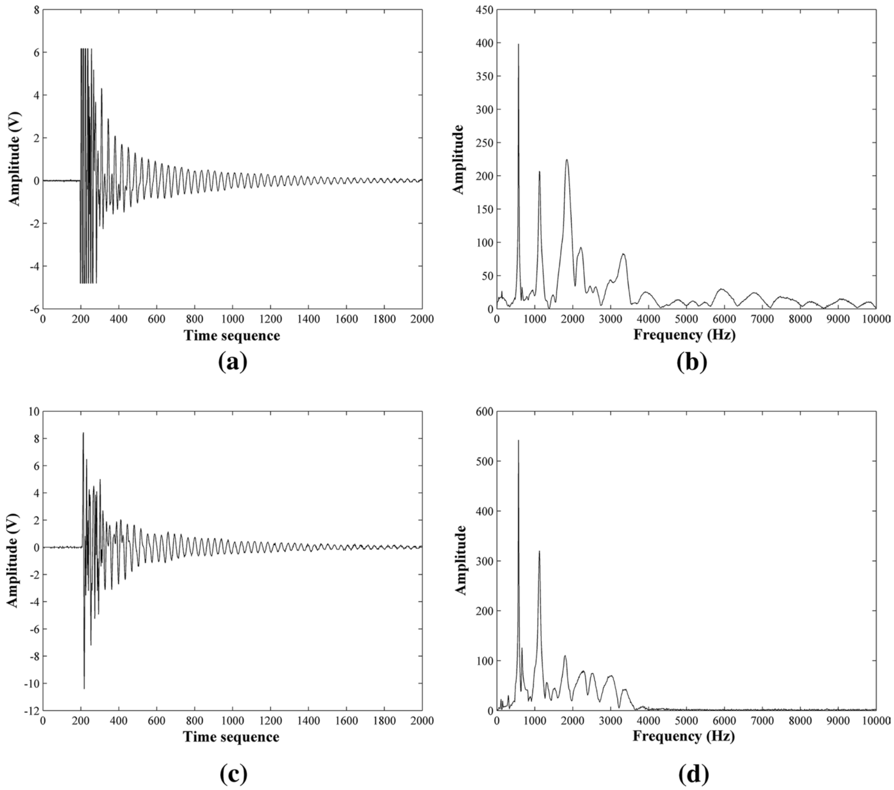

Fig. 4 Comparison diagram of the waveforms of response signals received from the impact end and the opposite end (log no. 5). **a** Time history of the acoustic signal from the impact end; **b** frequency spectrum of the signal collected from the impact end; **c** time history of the acoustic signal from the opposite end; **d** frequency spectrum of the signal collected from the opposite end

were almost the same. However, because the sensor in the impact end was affected by the lateral disturbance from mechanical impacts, the response signals received from the impact end exhibited some degree of nonlinear distortions. Therefore, the response signal received from the opposite end of a log was analyzed to determine various acoustic predicting parameters, including time centroid (T_c), and the first-order and second-order damping ratios.

Longitudinal acoustic velocity (V)

Longitudinal acoustic velocity of the logs can be obtained directly from the impact test using the Hitman HM200TM, a handheld resonance acoustic tool. Following the hammer impact, the tool immediately processed the response signal through a built-in fast Fourier transform (FFT) program (Harris et al. 2002; Wang et al. 2009). Acoustic velocity (V) is derived using the following equation:

$$V = \frac{2f_n L}{n} \tag{1}$$

where V is longitudinal acoustic velocity (m/s) of a log, f_n is the nth-order harmonic frequency (Hz) of the response signal, L is an end-to-end length (m) of a log, and n is the order of harmonic frequency.

Time centroid (T_c)

Time centroid, sometimes referred to as "mean time," represents the time when the bulk of the signal is received. Mathematically, T_c is obtained by dividing the first moment of the signal by the zeroth moment of the signal:

$$T_c = \frac{\sum_{i=1}^{N} |A_i| t_i}{\sum_{i=1}^{N} |A_i|}, \tag{2}$$

where N is the number of time samples, A_i is the amplitude of the ith time step, and t_i is the time at the ith time step. In general, when a signal is excited and transmitted in a flawless medium, most of its energy is typically located in the beginning of the signal waveform. Reflection and mode changes of the signal often come from the boundaries and material flaws, causing skewing of the signal in the time domain. As a form of the first moment analysis, time centroid has been widely used to characterize the damage or deterioration of materials (Titta et al. 1998; Bayissa et al. 2008).

Damping ratio (ζ) based on continuous wavelet transform

The continuous wavelet transform (CWT) of a finite energy signal $x(t) \in L^2(R)$ can be defined as (Mallat 1999)

$$W[x](a,b) = \frac{1}{\sqrt{a}} \int_{-\infty}^{+\infty} x(t) \varphi^* \left(\frac{t-b}{a} \right) \mathrm{d}t, \tag{3}$$

where $\varphi^*(\cdot)$ is the complex conjugate of the basic wavelet function $\varphi(\cdot)$, a and b are the dilation and translation parameters.

The most common wavelet for analyzing transient free vibration signals is the Morlet wavelet (Ruzzene et al. 1997; Chui 2006). In this paper, the modified Morlet wavelet is used to estimate the damping ratio of acoustic signal. A modified Morlet wavelet is defined as

$$\varphi(t) = \frac{1}{\sqrt{\pi f_b}} e^{j2\pi f_c t} e^{-t^2/f_b} \tag{4}$$

where f_b is the wavelet bandwidth parameter, f_c is center frequency. The Fourier transform of the Morlet wavelet is

$$\hat{\varphi}(af) = e^{-\pi^2 f_b (af - f_c)^2}. \tag{5}$$

It is assumed that the signal $x(t)$ is narrowband and asymptotic, and it can be described as a function of an instantaneous amplitude $A(t)>0$ and a phase $\psi(t)$ as follows (Le and Paultre 2013; Ülker-Kaustell and Karoumi 2011; Delprat et al. 1992)

$$x(t) = A(t)\cos(\psi(t)). \tag{6}$$

The CWT of the signal $x(t)$ can be obtained approximately by using Taylor's formulae around $t=b$ as follows (Chui 2006; Le and Paultre 2013; Delprat et al. 1992; Carmona et al. 1998)

$$W[x](a,b) \approx \frac{\sqrt{a}}{2}A(b)e^{j\psi(b)}\hat{\varphi}^*(a\dot{\psi}(b)), \tag{7}$$

where $\dot{\psi}(b)$ represents the time derivative of the phase, i.e., the instantaneous circular frequency.

According to the wavelet ridge theory, the maximum modulus of the CWT will be constricted to a curve in time–frequency plane, the curve is referred to as wavelet ridge $a_r(b)$, and the modulus $W[x]\left(a_r(b), b\right.$ corresponding to the points located in the curve is called wavelet skeleton. A definition of wavelet ridge and its skeleton is given as follows:

$$\begin{cases} a_r(b) = \omega_{\varphi_0}/\dot{\psi}(b) \\ W[x]\left(a_r(b), b\right) \approx \left(\sqrt{a}/2\right)A(b)e^{j\psi(b)}\hat{\varphi}^*\left(a_r(b)\dot{\psi}(b)\right) \end{cases}. \tag{8}$$

For a linear n-degree-of-freedom system, as the system is impacted by a unit impulse force, the response signal $x(t)$ can be represented as

$$x(t) = \sum_{i=1}^{n} A_i e^{-2\pi\zeta_i f_i t}\sin\left(2\pi f_{di}t\right), \quad t \geq 0, \tag{9}$$

where A_i is a constant only related to the testing point and modal order i, ζ_i is damping ratio of ith-order modal shape, f_i is ith-order undamped frequency, and $f_{di} = \sqrt{1-\zeta_i^2 f_i}$ is ith-order damped frequency.

When the Morlet wavelet transform is applied to $x(t)$, the following equation can be obtained according to Eqs. 5, 7, and 9

$$W[x](a,b) = \left(\sqrt{a}/2\right)\sum_{i=1}^{n} A_i e^{-2\pi\zeta_i f_i b}e^{-\pi^2 f_b\left(af_i - f_c\right)^2}e^{j\left(2\pi f_{di}b\right)}. \tag{10}$$

For a fixed value of the dilatation parameter $a=a_i=f_c/f_i$, by the definition of wavelet ridge and skeleton (see Eq. 8), the CWT of each separated mode i can be represented as

$$W[x]\left(a_i, b\right) = \frac{\sqrt{a_i}}{2}A_i e^{-2\pi\zeta_i f_i b}e^{j\left(2\pi f_{di}b\right)}. \tag{11}$$

For an idiomatic expression, t is substituted for b in above equation, and thus, the equation can be rewritten as

$$W[x](a_i, t) = \frac{\sqrt{a_i}}{2} A_i e^{-2\pi\zeta_i f_i t} e^{j(2\pi f_{di} t)} = B_i(t) e^{j\psi_i(t)}. \tag{12}$$

The instantaneous amplitude $B_i(t)$ and phase $\psi_i(t)$ can be defined as

$$\begin{cases} B_i(t) = \frac{\sqrt{a_i}}{2} A_i e^{-2\pi\zeta_i f_i t} \\ \psi_i(t) = 2\pi f_{di} t \end{cases}. \tag{13}$$

The following formulae can be obtained by taking the derivatives of Eq. 13

$$\begin{cases} \frac{\mathrm{d} \ln B_i(t)}{\mathrm{d}t} = \frac{1}{B_i(t)} \frac{\mathrm{d}B_i(t)}{\mathrm{d}t} = -2\pi\zeta_i f_i \\ \frac{\mathrm{d}\psi_i(t)}{\mathrm{d}t} = 2\pi f_{di} = 2\pi f_i \sqrt{1 - \zeta_i^2} \end{cases}. \tag{14}$$

The instantaneous frequencies f_i and damping ratios ζ_i of the system can be derived by solving Eq. 14.

Results and discussion

Physical characteristics of the hardwood log samples

The moisture content (MC) of the hardwood log samples ranged from 31.3 to 95.6% based on the MC disk measurements (Table 1). All logs were above the fiber saturation point (30% MC). Therefore, the logs tested were considered in green condition at the time of testing and the acoustic parameters discussed in this paper are treated as "green log" parameters.

Stress wave transit time in radial direction was mapped along the length of each log and is shown in Fig. 5 by species. Two black cherry logs (no. 1 and no. 5) had relatively low and consistent transit times (633–712 µs/m) along the length indicating generally sound internal condition, except log no. 5 showed slightly higher than normal transit time at locations 1–3. This observation was consistent with the visual appearances of these logs. The stress wave transit times in all other logs showed large variations along the length and among the logs and species, implying a wide range of physical conditions of these logs.

Because variation of transit times exists even in intact logs as a result of natural property variation, it is difficult to determine a single reference transit time for data interpretation. In this study, the lowest transit time in each individual log was used as a reference to determine the conditions in other locations. Specifically, it was aimed to determine the extent of internal decay, void, or other structural defects in each log based on the transit time maps and guide the process of dissecting logs for revealing actual physical conditions.

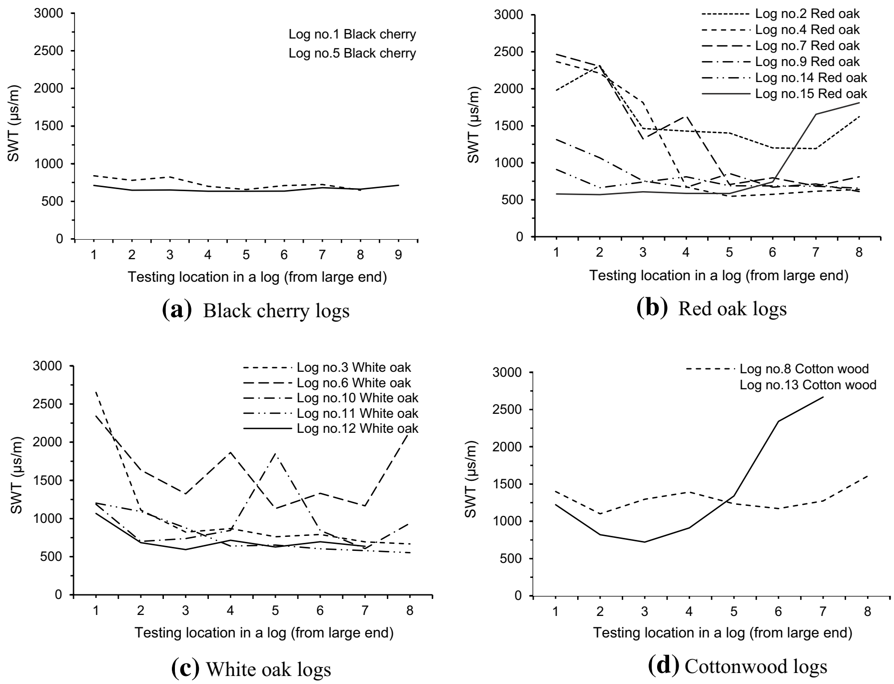

Fig. 5 Distribution of stress wave transit time (μs/m) in radial direction of hardwood logs

Based on the ground-truth defect maps created by dissecting at multiple locations and measuring the defected areas on each cross section, the defect ratio (k) of the log samples was found to range from 0 to 32%. The fifteen hardwood log samples were classified into five classes based on the defect ratio, as shown in Fig. 6. Two logs (no. 1 and no. 8) were identified as "solid logs" with no defects ($k=0$); two logs (no. 5 and no. 15) had minor defects ($k<5\%$); four logs (no. 4, no. 7, no. 12, no. 13) had moderate defects ($5\% \leq k < 10\%$); four logs (no. 3, no. 9, no. 10, and no. 14) had severe defects with defect ratio in the range of 10–20%; and three logs (no. 2, no. 6, and no. 11) had the most severe defects ($k \geq 20\%$).

It should be noted that log no. 8 (cottonwood) is a special case, i.e., all longitudinal acoustic parameters (V, T_c, ζ_1, and ζ_2) implied that log could be a sound log. However, stress wave transit time in radial direction was found in the range of 1101 to 1607 μs/m (Fig. 5d), significantly higher than the reference transit time (721 μs/m) of the other cottonwood log (no. 13), which indicated an abnormal internal condition. Close examination of the opened cross sections of log no. 8 revealed that a ring shake (separation or crack that runs parallel to the annual rings) existed in the boundary of heartwood and sapwood through the entire length of the log (see Fig. 7). Clearly, this ring shake has caused significant delay in arrival time, resulting in higher than normal transit times. On the other hand, in longitudinal impact testing of the same log, two sensors recording the response signals were located within the heartwood zone and close to the center of the end grain, and the ring shake did not

Fig. 6 Hardwood log classes based on defect ratio

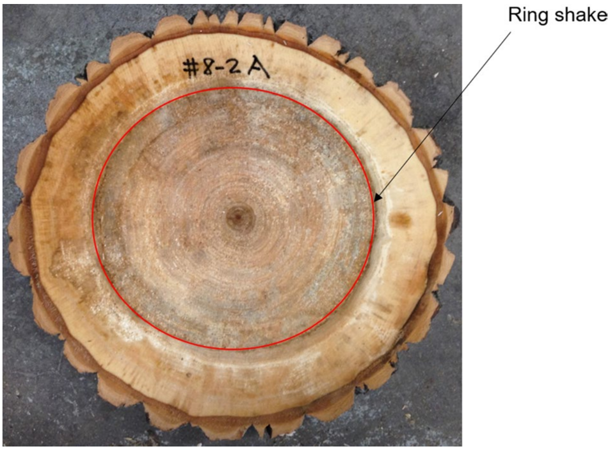

Fig. 7 Ring shake existed in cottonwood log no. 8

directly disrupt the longitudinal wave propagation. Consequently, the longitudinal acoustic parameters still reflect the solid wood condition. The implication of this phenomenon is that longitudinal acoustic impact testing is not sensitive to the presence of ring shakes within a log and therefore it will not identify this kind of defect.

Relationship between defect ratio and acoustic velocity

Table 2 shows various acoustic measures of the response signals. Acoustic velocity of the mixed species logs ranged from 2047 to 3317 m/s with a coefficient of variation (COV) of 14.3%. If logs were divided into five classes based on the defect ratios, the average acoustic velocity corresponding to each defect class was then observed as shown in Table 3. The small sample size of the logs in each class does not lend to a meaningful statistical comparison among classes, but the decreasing trend of acoustic velocity with increasing defect ratio is obvious.

Figure 8a shows the data plot of defect ratio and acoustic velocity for all fifteen hardwood logs tested. The relationship between defect ratio and velocity can be best described by a polynomial regression model,

$$k(\%) = 177.51 - 0.10V + 1.52E - 05V^2 \quad \left(R^2 = 0.72\right. \tag{15}$$

When the species and MC effect were disregarded, it appeared that as the log velocity dropped below 3000 m/s, the severity of internal decay increased in a much higher rate as log velocity continuously decreased.

Among the four hardwood species in the log samples, red oak had the largest sample size, with 6 logs. When red oak logs were examined alone, a similar decreasing trend of acoustic velocity with increasing defect ratio was observed (Fig. 8b). However, a power model was found to best fit the data mathematically ($R^2=0.76$). It is possible that species could have an effect on the defect ratio and acoustic velocity relationships.

Relationship between defect ratio and time centroid

The time centroid of fifteen hardwood logs ranged from 0.0165 to 0.0266 s, with a COV of 14.3%, the same COV as that of acoustic velocity. The T_c value was lower in sound logs than that in unsound logs. Figure 9 shows the data plot of log defect ratio and time centroid of fifteen hardwood logs. A good positive relationship was observed between defect ratio and time centroid, with the coefficient of determination (R^2) of 0.87 for a second-order polynomial regression. With this improved correlation, the time centroid of the acoustic response signal proved to be a better predictor of log defect ratio than log longitudinal acoustic velocity.

Estimation of damping ratio

The estimated damping ratios for all hardwood logs are summarized in Table 2. Figure 10 illustrates the procedures for estimating another important acoustic measure, damping ratio, of the hardwood logs, using log no. 1 (black cherry) as an example. Figure 10a shows the response signal of log no. 1. In the signal analysis, all response signals had been preprocessed through median filtering and a singular-value decomposition method (Xu and Liu 2011) to eliminate the noise that could

Table 2 Acoustic measures of the response signals received from the hardwood logs

Log no.	Species ID	Velocity V (m/s)	Time centroid T_c (s)	Scale s_1	First-order freq.[a] f_1 (Hz)	First-order damping ratio ζ_1	Scale s_2	Second-order freq.[b] f_2 (Hz)	Second-order damping ratio ζ_2
1	Black cherry	3250	0.017	143	699.3	0.019	74	1351.4	0.028
2	Red oak	2047	0.024	250	400.0	0.099	117	854.7	0.091
3	White oak	2697	0.023	193	518.1	0.063	96	1041.7	0.057
4	Red oak	3273	0.017	137	729.9	0.035	76	1315.8	0.027
5	Black cherry	3000	0.019	175	571.4	0.030	89	1123.6	0.036
6	White oak	2290	0.027	218	458.7	0.054	115	869.6	0.087
7	Red oak	2600	0.022	204	490.2	0.042	100	1000.0	0.047
8	Cottonwood	3317	0.017	150	666.7	0.021	74	1351.4	0.027
9	Red oak	2320	0.022	217	460.8	0.049	114	877.2	0.064
10	White oak	2790	0.021	173	578.0	0.049	89	1123.6	0.049
11	White oak	2460	0.024	208	480.8	0.044	106	943.4	0.061
12	White oak	2667	0.019	168	595.2	0.036	87	1149.4	0.037
13	Cottonwood	2700	0.018	151	662.3	0.037	83	1204.8	0.043
14	Red oak	2420	0.020	210	476.2	0.043	111	900.9	0.042
15	Red oak	3080	0.019	167	598.8	0.036	86	1162.8	0.034

[a,b] $f_i = \frac{f_c \times f_s}{s_i}$, where f_c is the central frequency of complex Morlet wavelet, f_s is the sampling frequency, and s_i and f_i are scale and its corresponding frequency of wavelet transform, respectively

Table 3 Corresponding relationship of log class, defect ratio (k), and average velocity (V)

Log class no.	Defect ratio k (%)	Average velocity V (m/s)
1	$k=0$	3284
2	$0<k<5$	3040
3	$5\leq k<10$	2810
4	$10\leq k<20$	2557
5	$20\leq k$	2266

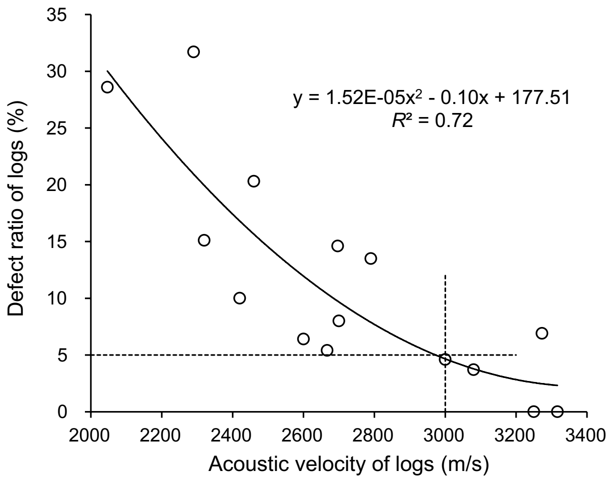

(a) Mixed species

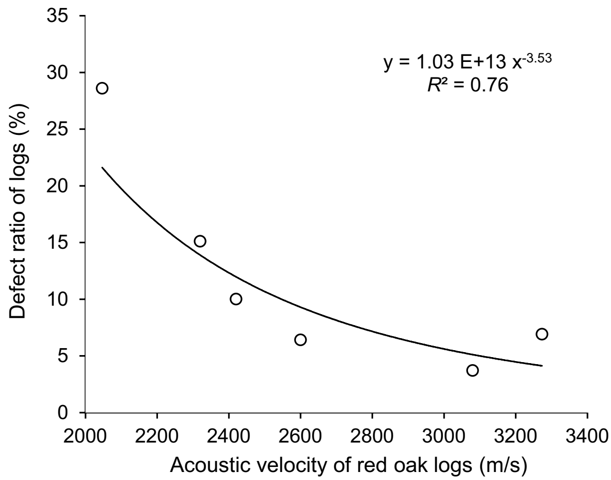

(b) Red oak

Fig. 8 Relationships between log defect ratio and log acoustic velocity of hardwood logs

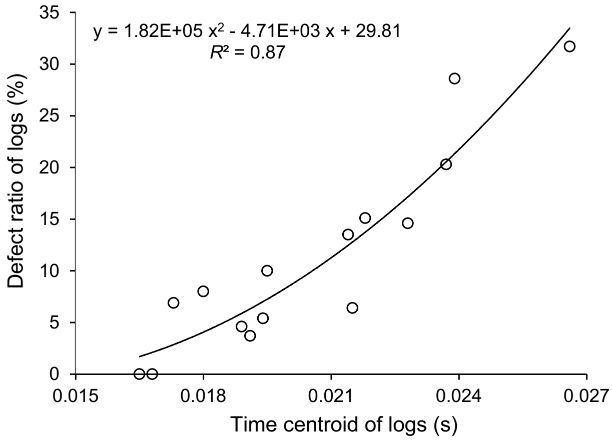

Fig. 9 Relationships between defect ratio and time centroid of hardwood logs

cause distortions to the derivatives of the skeletons. The distorted derivatives could directly affect the estimation of instantaneous frequency and damping ratio.

The wavelet moduli were obtained through CWT using a modified complex Morlet wavelet function (Eq. 4). They are shown in Fig. 10b in the form of two-dimensional contour map and in Fig. 10c in the form of three-dimensional mesh map. The wavelet ridge and skeleton were then calculated using Eq. 8 and are shown in Fig. 10b, c. Figure 10e, g shows the instantaneous scale (frequency) and damping ratio of the response signals through solving Eq. 14 (note: an inverse proportional relationship exists between frequency and scale). The instantaneous frequencies obtained were instantaneous natural frequency and the second-order harmonic frequency. The damping ratios discussed in this paper are therefore referred to as both the first mode and second mode.

Figure 10e shows the case of a high-quality log with no defects (log no. 1), where the instantaneous frequency did not vary much within the finite duration of the response signal, implying that the reflection and refraction of acoustic waves that are typically associated with internal defects did not exist. As a result, the estimated damping ratio deduced from the instantaneous frequency did not vary significantly. However, in the case of low-quality logs, such as log no. 2 (red oak) with severe internal rot and void ($k = 28.6$), variation of damping ratio was evident. For ease of use, a high-order polynomial fitting was performed on damping ratio data and the fitting curve (dashed line) is also shown in Fig. 10e.

Relationship between defect ratio and the first-order damping ratio

Figure 11 shows the data plot of defect ratio and first-order damping ratio of the hardwood logs. The regression result indicated a moderate linear relationship ($R^2 = 0.65$), with two seemingly outliers (logs no. 6 and no. 11). Examining the dissected cross sections of these two logs, it was found that they both contained a big single void that extended throughout the entire length in log no. 6 and 182 cm in log no. 11, resulting in a defect ratio of 31.7% (no. 6) and 20.3% (no. 11), respectively. The voids in these logs were concentrated in the heartwood, while the sapwood was left relatively intact. Although the acoustic velocity in these two logs was reduced significantly as a result of the center rot, the acoustic energy was still effectively transferred through the solid sapwood path, and the energy dissipation due to the center void was much less than that we would expect from a log with such a high defect ratio. As a result, the corresponding damping ratios were smaller than we expected from logs with such high defect ratios.

Another factor that might have influenced the damping ratio is moisture content of the logs. In Fig. 11, log no. 6 exhibited the largest deviation of damping ratio from the linear regression model. It turned out that log no. 6 had the lowest moisture content (31.3%) among all the hardwood logs tested. The drier wood of log no. 6 could have contributed to the low damping ratio value observed.

Based on the observed relationship between defect ratio and first-order damping ratio and the above analysis, it could be concluded that the first-order damping ratio not only depends on the size and volume of defects, but also related to wood MC, and how defects are distributed within a log.

Relationships between defect ratio and the second-order damping ratio

In theory, the second-order harmonic frequency component of the response signal has higher frequency and shorter wavelength; thus, it is more sensitive to the presence of smaller defects. In addition, it is understood that the higher the frequency and higher logarithmic decrement of the signal, the larger the corresponding damping ratio, which is more sensitive to the signal attenuation caused by defects (Thomson and Dahleh 1998). Based on the above analysis, the second-order damping ratio derived from the second-order frequency components could more accurately reflect the internal physical condition in logs than that through using the first-order damping ratio.

Similar to analysis of the first-order damping ratio, a linear regression analysis was also performed between the second-order damping ratio and log defect ratio as shown in Fig. 12. The results indicated that the second-order damping ratio had an excellent linear relationship with the log defect ratio ($R^2 = 0.92$). Comparing to the first-order damping ratio, the second-order damping ratio appeared not affected by the types of defects and how they were distributed in a log, and not sensitive to moisture content changes (e.g., log no. 6), but only relevant to the extent of the damage. Therefore, the second-order damping ratio of the response signal can characterize the defect condition of hardwood logs more accurately than the first-order damping ratio.

Comparing to the acoustic velocity of a log, second-order damping ratio predicted the degree of damage in a log more accurately and was not influenced by species.

Fig. 10 Illustration of procedures for estimating damping ratio of acoustic signals (log no. 1). **a** Time history of the acoustic signal; **b** timescale distribution of wavelet modulus and ridge of the acoustic signal obtained through CWT; **c** timescale distribution of wavelet modulus and skeleton; **d** fundamental frequency component of the acoustic signal and its skeleton; **e** instantaneous scale (frequency), damping ratio and fitted damping ratio curve based on fundamental frequency component of the signal; **f** second-order harmonic component of acoustic signal and its skeleton; **g** instantaneous scale (frequency), damping ratio, and fitted damping ratio curve based on the second-order harmonic component of the signal ▶

Defect prediction models based on multiple acoustic parameters

Individual acoustic parameters including acoustic velocity, time centroid, and damping ratios showed moderate-to-good correlations with the defect ratio of hardwood logs. For the purpose of practical application, these individual parameters can be used in combination to obtain optimal prediction. Therefore, multivariate regression analysis was conducted to examine the predicting strength of various combinations of acoustic velocity, time centroid, and the first- and second-order damping ratios.

The multivariate prediction models examined are in nonlinear polynomial form:

$$k(\%) = b_0 + b_1x_1 + b_2x_2 + b_3x_3 + b_4x_4 + b_5x_1^2 + b_6x_2^2, \quad (16)$$

where x_1, x_2, x_3, and x_4 are individual acoustic predicting variables V, T_c, ζ_1, and ζ_2, respectively. b_0, b_1, b_2, b_3, b_4, b_5, and b_6 are regression coefficients.

Because of the linear nature of the damping ratio and defect ratio relationships, the higher order of the variables was not considered for damping ratios. Table 4 shows the results of multivariate regression analysis for predicting defect ratio of hardwood logs. Compared to the single-parameter prediction models of individual V, T_c, and ζ_1, the multiple parameter prediction models have generally increased the prediction power as evidenced by the increase in the determination coefficient (R^2) and decrease in the root mean squared error (RMSE). It is also clear that certain parameter combinations yielded limited improvement in the regression results.

In addition, multivariate regression analyses indicated that the second-order damping ratio (ζ_2) and time centroid (T_c) are the two most important acoustic parameters representing the internal defect of hardwood logs. As seen in Table 4, the optimal model for predicting or evaluating the internal defect of hardwood logs could be derived from the combination of multiple parameters of T_c, ζ_1, and ζ_2 or of V, T_c, and ζ_1. However, considering the accuracy of prediction and simplicity of analysis, the second-order damping ratio could be the best single predictor for assessing internal soundness of hardwood logs.

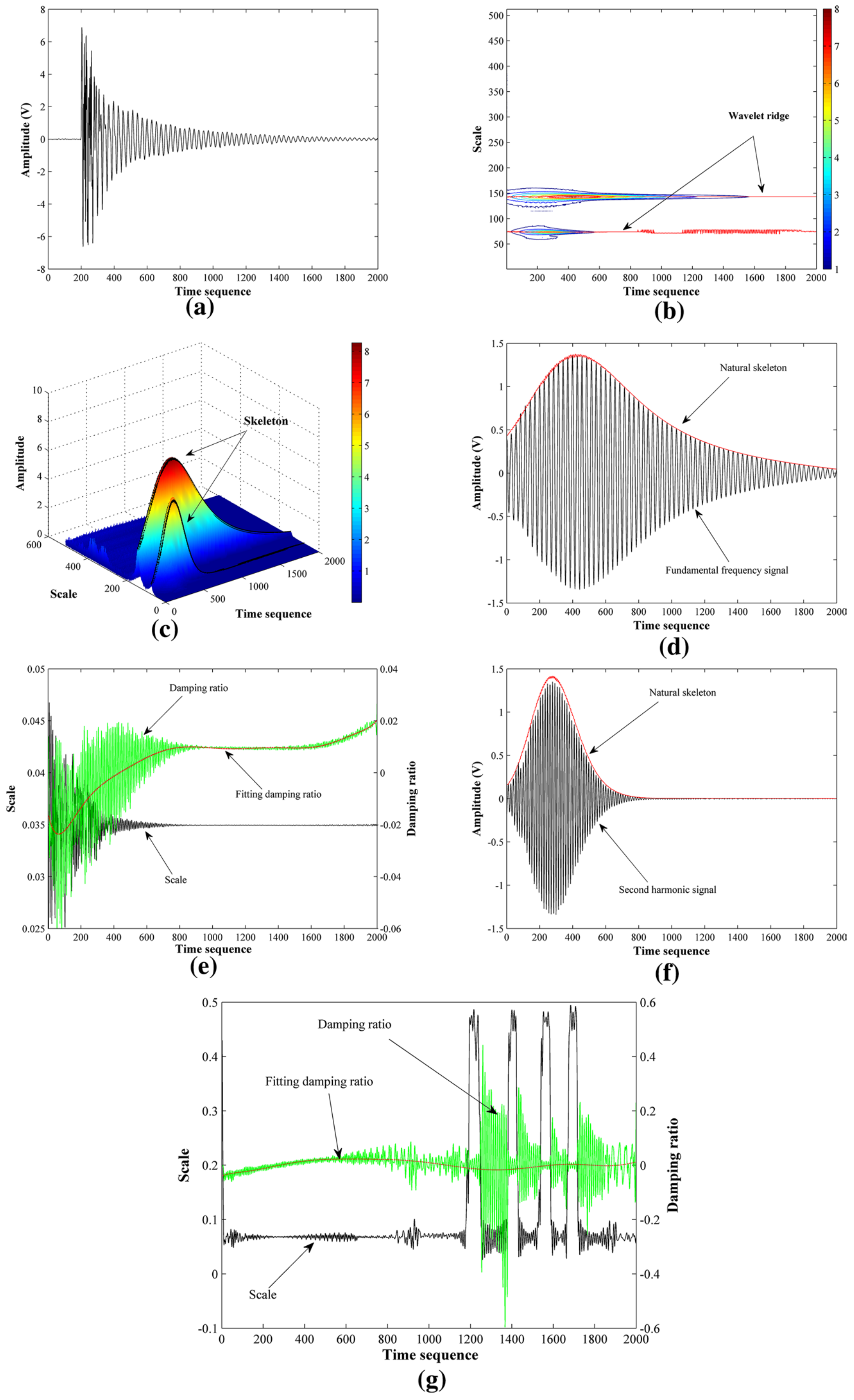
Amplitude (V)
Time sequence
(a)
Wavelet ridge
Scale
Time sequence
(b)
Skeleton
Amplitude
Scale
Time sequence
(c)
Natural skeleton
Fundamental frequency signal
Amplitude (V)
Time sequence
(d)
Damping ratio
Fitting damping ratio
Scale
Damping ratio
Time sequence
(e)
Natural skeleton
Second harmonic signal
Amplitude (V)
Time sequence
(f)
Damping ratio
Fitting damping ratio
Scale
Damping ratio
Time sequence
(g)

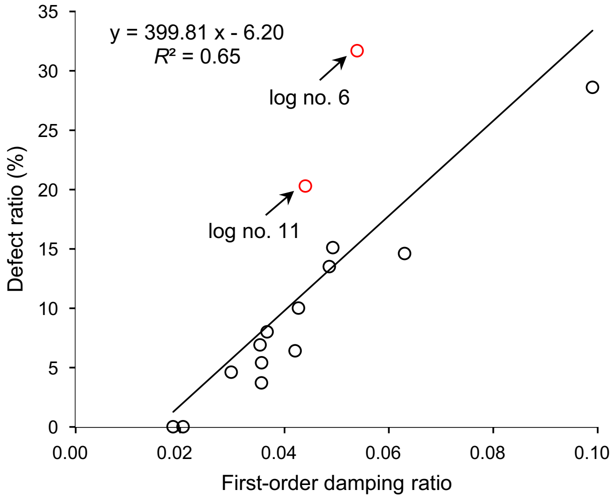

Fig. 11 Relationship between defect ratio and the first-order damping ratio of the hardwood logs

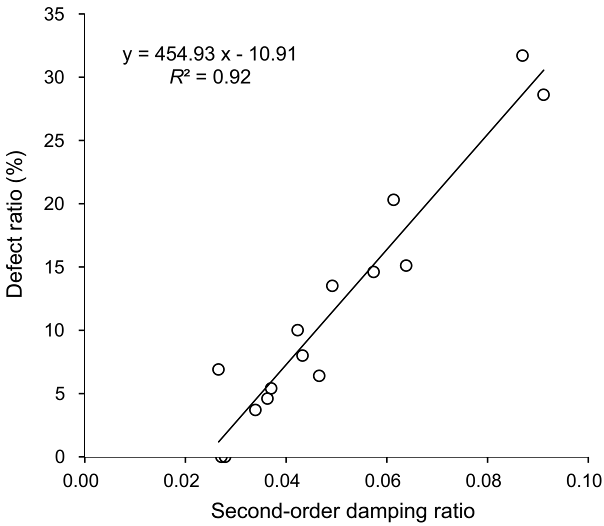

Fig. 12 Relationship between defect ratio and the second-order damping ratio of the hardwood logs

Table 4 Regression of defect ratio on acoustic velocity (V), time centroid (T_c), first-order damping ratio (ζ_1), second-order damping ratio (ζ_2), and the combination of V, T_c, ζ_1, and ζ_2

Predictors				Coefficients							Regression statistic		
x_1	x_2	x_3	x_4	b_0	b_1 (x_1)	b_2 (x_2)	b_3 (x_3)	b_4 (x_4)	b_5 (x_1^2)	b_6 (x_2^2)	R^2	Adjusted R^2	RMSE
V	–	–	–	177.51	−103.07	–	–	–	15.15	–	0.72	0.68	29.56
T_c	–	–	–	29.81	−4.71	–	–	–	0.18	–	0.87	0.85	13.66
ζ_1	–	–	–	−6.21	400.05	–	–	–	–	–	0.65	0.63	34.13
ζ_2	–	–	–	-10.93	455.30	–	–	–	–	–	0.92	0.92	7.38
V	T_c	–	–	137.06	−68.01	−4.50	–	–	11.07	0.16	0.93	0.90	8.72
V	ζ_1	–	–	104.93	−61.18	168.40	–	–	8.68	–	0.76	0.69	28.01
V	ζ_2	–		−36.19	13.33	513.61	–	–	−1.84	–	0.93	0.91	8.34
T_c	ζ_1	–	–	75.78	−9.06	195.46	–	–	0.26	–	0.94	0.92	7.14
T_c	ζ_2	–		27.89	−4.04	332.54	–	–	0.12	–	0.94	0.93	6.60
ζ_1	ζ_2	–	–	−10.85	−20.47	471.96	–	–	–	–	0.93	0.91	7.94
V	T_c	ζ_1	–	118.35	−5.22	−11.19	159.98	–	−0.06	0.30	0.95	0.92	6.95
V	T_c	ζ_2	–	53.88	−17.34	−3.99	269.38	–	2.86	0.12	0.94	0.91	7.94
V	ζ_1	ζ_2	–	−34.22	12.11	−10.13	519.36	–	−1.64	–	0.93	0.90	9.16
T_c	ζ_1	ζ_2	–	51.20	−6.43	96.06	208.46	–	0.18	–	0.95	0.93	6.47
V	T_c	ζ_1	ζ_2	89.62	2.71	−9.75	130.18	104.34	−1.17	0.26	0.95	0.92	7.63

Conclusion

In this study, the potential of an acoustic impact testing method for evaluating the soundness of hardwood logs was investigated. In addition to examining longitudinal acoustic velocity and time centroid as single predictors of defect ratio, a continuous wavelet transform (CWT)-based method was used to determine the first- and second-order damping ratios, and their relationships with the extent of internal defect in hardwood logs. The potential of using a combination of acoustic velocity, time centroid, and damping ratios to improve the defect prediction was also determined through multivariate regression analysis. Based on the results and analysis, the following conclusions were drawn:

1. Acoustic velocity measured in hardwood logs was negatively affected by the internal defects of the logs. Log acoustic velocity generally decreased with increasing severity of internal defects. When log velocity dropped below a critical value, the severity of internal decay increased at a much higher rate as log velocity continuously decreased. This critical velocity value can be different for different species, but 3000 m/s can be used as a threshold for logs of mixed species.
2. Time centroid of the response signals was positively affected by internal defects of hardwood logs, and it proved to be a better predictor of log defect ratio than log acoustic velocity.
3. Damping ratios of the response signals have linear and positive relationships with log defect ratio. Comparing to the first-order damping ratio, the second-order damping ratio appeared not affected by wood moisture content and how defects were distributed in a log. The second-order damping ratio can characterize the defect condition of hardwood logs more accurately than the first-order damping ratio.
4. The optimal model for predicting internal defect of hardwood logs could be derived from combinations of multiple acoustic parameters. However, considering both the accuracy of prediction and simplicity of analysis, the second-order damping ratio could be the best single predictor for assessing internal soundness of hardwood logs.

The hardwood logs examined in this study contained a wide range of deterioration levels, which were difficult to quantify with precision. The response signals from impact testing of the logs were complex and variable. Although the results and analysis indicated a very good potential of using the impact testing method, coupled with advanced signal analysis, to predict the existence and extent of internal defects in hardwood logs, large-scale experiments with commercial-size logs need to be carried out in future to test the feasibility and applicability of the acoustic impact test technique in production lines.

Acknowledgements This research was conducted through research cooperation between the USDA Forest Service Forest Products Laboratory (FPL) and Nanjing Forestry University (NFU), China, and was supported in part by the National Natural Science Foundation of China (Grant No. 31170668), the Priority Academic Program Development (PAPD) of Jiangsu Higher Education Institutions, and the NFU

Innovation Grant for Outstanding PhD Dissertations (Grant No. 163070682). The authors acknowledge the technical support from the Engineering Mechanics and Remote Sensing Laboratory (EMRSL) at the FPL.

Compliance with ethical standards

Conflict of interest On behalf of all authors, the corresponding authors state that there is no conflict of interest.

References

Addis T, Buchanan AH, Walker JCF (1997) Log segregation into stiffness classes. In: Ridoutt BG (ed) Managing variability in resource quality. FRI Bulletin No. 202, Forest Research Institute, Rotorua, pp 7–10

Addis T, Buchanan AH, Walker JCF (2000) Selecting trees for structural timber. Holz Roh-Werkst 58(3):162–167

ASTM (2003) Standard test methods for direct moisture content measurement of wood and wood-base materials. ASTM D4442-92. America Society for Testing and Materials, Philadelphia, PA

Bayissa WL, Haritos N, Thelandersson S (2008) Vibration-based structural damage identification using wavelet transform. Mech Syst Signal Process 22(5):1194–1215

Carmona R, Hwang WL, Torrésani B (1998) Practical time–frequency analysis: Gabor and wavelet transforms with an implementation in S. Academic Press, San Diego

Carter P, Lausberg M (2003) Application of Hitman acoustic technology—the Carter Holt Harvey experience. FIEA paper, p 6

Carter P, Briggs D, Ross RJ, Wang X (2005) Acoustic testing to enhance western forest values and meet customer wood quality needs. PNW-GTR-642. In: Harrington CA, Schoenholtz SH (eds) Productivity of western forests: a forest products focus. USDA Forest Service, Pacific Northwest Research Station, Portland, OR, pp 121–129

Chui C (2006) An introduction to wavelets. Academic Press, San Diego

Delprat N, Escudié B, Guillemain P, Kronland-Martinet R, Tchamitchian P, Torrésani B (1992) Asymptotic wavelet and Gabor analysis: extraction of instantaneous frequencies. IEEE Trans Inf Theory 38(2):644–664

Essien C, Via BK, Cheng Q, Gallagher T, McDonald T, Wang X, Eckhardt LG (2017) Multivariate modeling of acoustomechanical response of 14-year-old suppressed loblolly pine (*Pinus taeda*) to variation in wood chemistry, microfibril angle and density. Wood Sci Technol 51:475–492

Harris P, Petherick R, Andrews M (2002) Acoustic resonance tools. In: Proceedings 13th international symposium on nondestructive testing of wood, 19–21 Aug 2002, Berkeley, CA, pp 195–201

Huang CL, Londstrom H, Nakada R, Ralston J (2003) Cell wall structure and wood properties determined by acoustics—a select review. Holz Roh-Werkst 61:321–335

Le TP, Paultre P (2013) Modal identification based on the time-frequency domain decomposition of unknown-input dynamic tests. Int J Mech Sci 71:41–50

Mallat S (1999) A wavelet tour of signal processing, 2nd edn. Academic Press, San Diego

Pellerin RF, DeGroot RC, Esenther GR (1985) Nondestructive stress wave measurements of decay and termite attack in experimental wood units. In: Proceedings, 5th nondestructive testing of wood, September 9–11, 1985, Pullman, WA. Washington State University, Pullman, WA, pp 319–353

Ross RJ, Wang X, Brashaw BK (2005) Inspection and monitoring techniques for bridges and civil structures. In: Fu G (ed) Detecting decay in wood component. Woodhead Publishing Limited, Cambridge, pp 100–114

Ruzzene M, Fasana A, Garibaldi L, Piombo B (1997) Natural frequencies and dampings identification using wavelet transform: application to real data. Mech Syst Signal Process 11(2):207–218

Steele PH, Harless TEG, Wagner FG, Kumar L, Taylor FW (1994) Increased lumber value from optimum orientation of internal defects with respect to sawing pattern in hardwood sawlogs. Forest Prod J 44(3):69–72

Thomas RE (2008) Predicting internal yellow-poplar log defect features using surface indicators. Wood Fiber Sci 40(1):14–22

Thomas RE (2010) Validation of an internal hardwood log defect prediction model. In: Fei et al. (eds) Proceedings of the 17th central hardwood forest conference, April 5–7, 2010, Lexington, KY. Gen. Tech. Rep. NRS-P-78. Newtown Square, PA: U.S. Department of Agriculture, Forest Service, Northern Research Station, pp 77–82

Thomson WT, Dahleh MD (1998) Theory of vibration with applications, 5th edn. Prentice-Hall, Inc., Upper Saddle River

Titta M, Beall FC, Biernacki JM (1998) Acousto-ultrasonic assessment of internal decay in glulam beams. Wood Fiber Sci 30(3):259–272

Ülker-Kaustell M, Karoumi R (2011) Application of the continuous wavelet transform on the free vibrations of a steel-concrete composite railway bridge. Eng Struct 33(3):911–919

Wang X, Ross RJ, Green DW, Brashaw B, Englund K, Wolcott M (2004) Stress wave sorting of red maple logs for structural quality. Wood Sci Technol 37(6):531–537

Wang X, Wiedenbeck J, Ross RJ, Forsman JW, Erickson JR, Pilon C, Brashaw BK (2005) Nondestructive evaluation of incipient decay in hardwood logs. Gen. Tech. Rep. FPL-GTR-162. USDA, Forest Service, Forest Products Laboratory, Madison, WI, pp 1–11

Wang X, Carter P, Ross RJ, Brashaw BK (2007) Acoustic assessment of wood quality of raw forest materials—a path to increased profitability. For Prod J 57(5):6–14

Wang X, Stelzer HE, Wiedenbeck J, Lebow PK, Ross RJ (2009) Assessing wood quality of borer-infested red oak logs with a resonance acoustic technique. Wood Fiber Sci 41(2):180–193

Wang X, Verrill S, Lowell E, Ross RJ, Herian VL (2013) Acoustic sorting models for improved log segregation. Wood Sci Technol 45(4):343–352

Wang X, Thomas E, Xu F, Liu Y, Brashaw BK, Ross RJ (2018) Defect detection and quality assessment of hardwood logs: part 2—combined acoustic and laser scanning system. Wood Fiber Sci 50(3):310–322

Xu F, Liu YF (2011) Feature extraction of acoustic emission signals based on median filter-singular value decomposition and empirical mode decomposition. Chin J Sci Instrum 32(12):2712–2719

Xu F, Wang X, Liu Y, Brashaw BK, Yeary LA (2017) Assessing internal soundness of hardwood logs by acoustic impact testing. In: Wang X, Senalik CA, Ross RJ (eds) Proceedings: 20th international nondestructive testing and evaluation of wood symposium. General technical report FPL-GTR-249. Madison, WI: U.S. Department of Agriculture, Forest Service, Forest Products Laboratory, pp 446–455

Xu F, Wang X, Thomas E, Liu Y, Brashaw BK, Ross RJ (2018) Defect detection and quality assessment of hardwood logs: part 1—acoustic impact test and wavelet analysis. Wood Fiber Sci 50(3):291–309

Affiliations

Feng Xu[1] · Yunfei Liu[1] · Xiping Wang[2] · Brian K. Brashaw[2] · Lon A. Yeary[3] · Robert J. Ross[2]

1 College of Information Science and Technology, Nanjing Forestry University, Nanjing 210037, China

2 Forest Products Laboratory, USDA Forest Service, 1 Gifford Pinchot Drive, Madison, WI 53726-2398, USA

3 Mississippi State University, Starkville, MS, USA